Effects of surface waves on the behavior of perfect lenses

Michael W. Feise, Peter J. Bevelacqua, and John B. Schneider
School of Electrical Engineering and Computer Science, Washington State University, Pullman, Washington 99164-2752
(Received 5 February 2002; revised manuscript received 23 May 2002; published 22 July 2002)

Backwards-wave (BW) materials, which have simultaneously negative permittivity and permeability, support electromagnetic waves with phase propagation in the direction opposite to power flow. At an interface between BW materials and free space, the normal component of the wave vector changes sign. In the case of an evanescent wave, this leads to growth of the field amplitude inside the BW material. An infinite slab of an ideal, homogeneous BW material can simultaneously compensate the phase and the amplitude propagation of a wave, such that a point source is perfectly reconstructed in the image [J. B. Pendry, Phys. Rev. Lett. **85**, 3966 (2000)]. However, it is more realistic to consider a thin layer at the surface over which the permeability and permittivity change from the free-space values to the BW values. Such layers influence the response of the system through a frequency shift of surface modes and the nonreflecting wave. One finds a lower bound for the size of resolvable features. It is shown that the transition layer is important even at thicknesses much smaller than the free-space wavelength of the radiation.

DOI: 10.1103/PhysRevB.66.035113 PACS number(s): 78.20.Ci, 42.30.Wb, 73.20.Mf, 78.66.−w

I. INTRODUCTION

Recently, materials that simultaneously have a negative electric permittivity and a negative magnetic permeability have received renewed attention. These materials can support a backwards-traveling wave where the phase propagation is antiparallel to the direction of energy flow. For this reason we identify these materials as backwards wave (BW) materials. The extraordinary properties of such materials have been predicted and theoretically studied by Veselago several decades ago,[1] but experimental realization had not been achieved until recently.[2] This type of material is predicted to possess unusual electromagnetic properties such as an inverse Doppler shift and a backwards-directed Cherenkov radiation cone. Veselago pointed out that a planar slab of BW material would refocus the waves from a point source.[1] Recently, Pendry predicted that the BW slab would also amplify the evanescent waves[3] and thus under certain conditions refocus the light to an exact image of the source. In imaging applications, the evanescent waves are crucial to resolve features smaller than the free-space wavelength of the electromagnetic radiation. Pendry's claim was further studied by Ziolkowski[4] who considered the consequences of lossy material and the behavior of fields whose frequencies were not ideal for the given material which is necessarily dispersive.

This paper presents results of calculations, using the macroscopic Maxwell equations, pertaining to the behavior of evanescent waves in BW materials. First, we briefly discuss an evanescent wave at the interface of free space and BW half spaces and an evanescent wave interacting with a slab of BW material. Then the theoretical analysis is described, and finally a more realistic model system where the transition from free space to BW material is finite in space is presented (i.e., there is an offset between the discontinuity in permittivity and permeability).

II. SINGLE AND DOUBLE INTERFACE CONSIDERATIONS

It can be shown that BW material, where both the permittivity and the permeability are simultaneously negative, can only be realized if the material is dispersive[1] (ε and μ will be used for the relative permittivity and permeability, respectively). Thus the ideal situation of $\varepsilon=\mu=-1$ is possible only at a finite number of frequencies. This set of parameter values is identified as ''ideal'' because it gives the same impedance and speed of light as free space.

Consider a monochromatic plane wave with wave vector **k** incident on an interface between free space and a BW half space. Let the BW material have $\varepsilon=\mu=-1$ at the frequency of the plane wave. Due to the impedance matching with free space, there is no reflected wave. The magnitude of all vector components are then unchanged at the interface because the speed of light has the same magnitude everywhere in the system. The boundary conditions require that the tangential components of **E** and **H**, as well as the normal components of **D** and **B**, are continuous across the interface. From the constitutive relations we then find that the normal components of **E** and **H** must change sign. Given the behavior of the fields at the boundaries, Maxwell's equations require that the tangential components of **k** are continuous, and its normal component changes sign. This result is independent of the fact that the vectors may be real, imaginary, or complex valued and there is no need to invoke causality, as was done in Refs. 3 and 4. In the case of a propagating wave, the phase velocity changes its direction normal to the interface, while for an evanescent wave that has the imaginary wave-vector component normal to the interface, the change of signs across the interface dictates that a decaying exponential on one side of the interface becomes a growing one on the other side (and vice versa).

Assume the BW material is a slab with interfaces to free space parallel to the x-z plane, and a source of plane waves is placed to one side of the slab. In general, due to reflections at the interfaces, both positive and negative values of the y component of the wave vector are present. However, for the special case where the frequency yields $\varepsilon=\mu=-1$, the slab is impedance matched to free space and one of these waves vanishes such that the phase and amplitude propagation reverse direction normal to the interfaces. For instance, an in-

cident decaying evanescent wave grows inside the BW slab and upon leaving the slab decays again. In this case there is only a single wave in each region. The magnitude of k_y is identical in all regions (subscripts denote vector components), and the slab compensates for the propagation over a distance in free space equal to the slab thickness, independent of wave vector. This configuration is ideal for construction of a ''perfect lens,'' where the phase propagation of a propagating wave and the amplitude propagation of an evanescent wave need to be compensated to achieve perfect focusing to a point.

In practice, a BW material has been realized as a periodic arrangement of split-ring resonators (SRR) and thin-wire modules that cause an effective dispersion of μ and ε similar to the permittivity of a plasma. The modules are anisotropic and to achieve better isotropy they are arranged in a pattern with modules facing in different directions,[5,6] i.e., one uses a periodic structure similar to a crystal. Due to the composite nature of the material there exists a displacement between the thin-wire module that causes the dispersion in ε and the SRR module that gives dispersion in μ. One might expect that this thin transition layer can be neglected, but due to multiple reflections at the interfaces and especially the amplification of evanescent waves in the BW slab, this thin layer can have important implications for the realization of a perfect lens.

III. THEORETICAL ANALYSIS

The following analysis employs the macroscopic Maxwell equations to find the behavior of the electromagnetic fields in the example geometry shown in Fig. 1. The same procedure can be applied to any layered dielectric system. Assume an incident transverse electric (TE) plane wave of the form

$$\mathbf{E}(x,y,t)=\hat{z}E_i e^{i(k_x x+k_y y-\omega t)} \tag{1}$$

in the region to the left of the slab, where E_i is the incident wave amplitude and k_x and k_y are the wave vector components. Let the media be linear, isotropic, and translationally invariant in the x and z direction. Linearity allows one to work in frequency space with a monochromatic wave, while isotropy lets the wave vectors in the different regions share the same plane of incidence. Therefore one can choose a coordinate system such that the x-y plane coincides with the plane of incidence and $k_z \equiv 0$ everywhere. At all interfaces reflections can occur and one has to allow for waves with both signs of k_y in the analysis. As there is no incident field from the right, the region to the right of the slab has only a single wave. The amplitude of the reflected wave to the left of the slab and that of the transmitted wave to the right is denoted as E_r and E_t, respectively. The waves in the different regions of the system are connected through the boundary conditions on the electromagnetic fields at the dielectric interfaces, namely the continuity of the tangential components of **E** and **H** and the normal components of **D** and **B**. The boundary conditions together with the dispersion relation in each region give two equations fewer than the number of wave-vector and field components. Thus one wave vector component (e.g., k_x) can be used to parametrize the direction of incidence; frequency is also used as a parameter. This still leaves an underdetermined system of equations with one equation fewer than unknowns. After a lengthy but straightforward calculation one can find solutions relating two field amplitudes, e.g., for the system of Fig. 1,

$$\frac{E_r}{E_i}=\frac{(k_y^{21})^2[e^{2iLk_y^{22}}(C_1^{22}+iS_2^{21})^2+(iC_1^{22}+S_2^{21})^2]-(k_y^{11})^2[e^{2iLk_y^{22}}(iS_1^{22}+C_2^{21})^2+(S_1^{22}+iC_2^{21})^2]}{e^{2idk_y^{11}}\{e^{2iLk_y^{22}}[(S_1^{11}+iC_1^{21})k_y^{22}-(iC_2^{11}+S_2^{21})k_y^{21}]^2-[(S_1^{11}+iC_1^{21})k_y^{22}+(iC_2^{11}+S_2^{21})k_y^{21}]^2\}}, \tag{2}$$

$$\frac{E_t}{E_i}=\frac{4e^{iL(k_y^{22}-k_y^{11})}k_y^{11}(k_y^{21})^2k_y^{22}\mu_1\mu_2}{e^{2idk_y^{11}}\{e^{2iLk_y^{22}}[(S_1^{11}+iC_1^{21})k_y^{22}-(iC_2^{11}+S_2^{21})k_y^{21}]^2-[(S_1^{11}+iC_1^{21})k_y^{22}+(iC_2^{11}+S_2^{21})k_y^{21}]^2\}}, \tag{3}$$

where $S_j^{mn}=k_y^{mn}\mu_j\sin(dk_y^{21})$, $C_j^{mn}=k_y^{mn}\mu_j\cos(dk_y^{21})$, the distances L and d are defined in the figure caption, and the dependence on ω and k_x is implicit through $k_y^{mn}(\omega,k_x)$, which is determined by the dispersion relation (k_x is equal in all regions)

$$\varepsilon_m(\omega)\mu_n(\omega)\omega^2=c_0^2\mathbf{k}^{mn}\cdot\mathbf{k}^{mn}, \tag{4}$$

where c_0 denotes the speed of light in vacuum. The first and second superscript on the wave vectors correspond to the subscript on the permittivity and permeability in each region, respectively. In this system the slab proper has superscript 22 and the surrounding space has superscript 11. On either side between the two is a transition layer with ε_2 and μ_1 giving superscript 21. If desired, one can write such relations for all the field amplitudes in the system. With one of the amplitudes as a reference parameter (the relations shown use E_i), one can calculate the fields at all points by taking into account the complex exponential in Eq. (1) and adding the respective waves at that point. Under certain conditions it is possible for the numerator in Eq. (2) or the denominator in Eq. (2) and (3) to vanish. This means that $E_r=0$ or $E_i=0$, respectively. When E_r vanishes, the system does not reflect the particular incident wave, while vanishing E_i signifies the existence of a bound mode. A bound mode can only exist if k_y is imaginary in both of the outside regions, otherwise there would be net energy flow out of the system without any sources. Thus it is characterized by the electric field outside

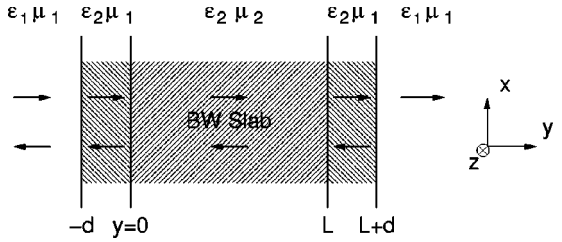

FIG. 1. Schematic of the infinite slab configuration. The slab has a thickness L and there is a transition layer of thickness d to either side. The system is translationally invariant in the x and z direction. Free-space quantities are denoted by a subscript 1 and dispersive material quantities by a subscript 2.

the system exponentially decaying away from the interface. Inside the slab the mode can be of propagating or evanescent character. A bound mode that is of evanescent character inside the slab has its field amplitude exponentially localized at the interfaces and is called a surface mode.

IV. MODEL CALCULATIONS

The previous section outlined the general theoretical analysis of a planar system with the example geometry of Fig. 1. This section characterizes the parameters used in the model system and presents calculations leading to an analysis of its imaging capabilities.

A. Model parameters

The materials considered here have the commonly-used relative permittivity

$$\varepsilon(\omega)=1-\frac{\omega_{ep}^2}{\omega^2}, \tag{5}$$

where ω_{ep} is the effective electrical plasma frequency. Analogously, for the relative permeability we use

$$\mu(\omega)=1-\frac{\omega_{mp}^2}{\omega^2}, \tag{6}$$

where ω_{mp} is the effective magnetic plasma frequency.[3,5] As the electric and magnetic plasma frequencies are available as design parameters of the BW composite material, we consider the special case of $\omega_{ep}=\omega_{mp}=\omega_p$ to simplify the model. We also have neglected damping. Thus the material behaves as a BW material for $\omega<\omega_p$ and has $\mu=\varepsilon=-1$ at $\omega=\omega_0=\omega_p/\sqrt{2}=c_0 2\pi/\lambda_0$.

Because of their importance in achieving a perfect focus, we concentrate our attention on the behavior of evanescent waves. Evanescent waves have a complex wave vector, whose real part is perpendicular to its imaginary part. The real part determines the wavelength λ_t of the wave transverse (perpendicular) to the direction of maximum amplitude decay. This wavelength determines the image resolution that can be achieved with this wave. For evanescent waves λ_t is always less than the free space wavelength. We assume an embedded source to the left of the slab with frequency ω_s. A schematic of the system is shown in Fig. 1; the system is translationally invariant in the x and z direction. The BW material slab has a length L and a transition layer of thickness d with the permittivity of the BW material but the permeability of free space exists to either side. In all following calculations $L=0.36\lambda_0$ and $\omega_0/(2\pi)=15$ GHz. Larger values of L have been investigated and found to be more restrictive for imaging purposes. The particular value for the frequency has been chosen to be close to the ones used in experiments,[5] but is not essential to the findings of this study.

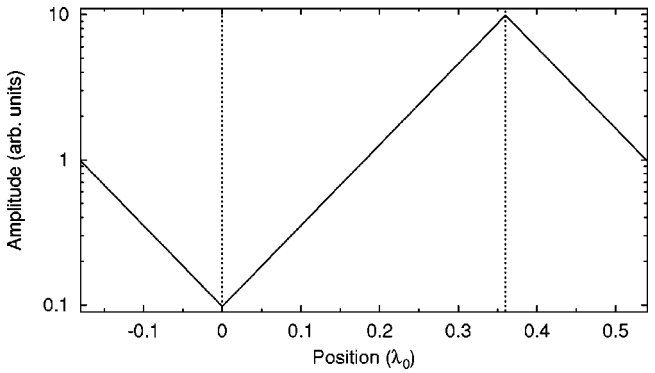

FIG. 2. Electric field amplitude of the nonreflecting evanescent wave in the system shown in Fig. 1 with vanishing transition-layer thickness $d=0$ at the design frequency $\omega_s=\omega_0$ and with $\lambda_t=0.44\lambda_s$. The dashed lines indicate the location of the slab surfaces. The plane-wave source is at an arbitrary location left of the slab ($y<0$).

The calculations to follow consider only evanescent waves that have maximum decay in the y direction and λ_t tangential to the interface. The x component of the wave vector is determined by the transverse wavelength through $k_x=2\pi/\lambda_t$; k_z is zero. The frequency and the components of the wave vector in each region are related through the respective dispersion relation.

B. Results and discussion

For the case of vanishing transition-layer thickness $d=0$ and design frequency $\omega_0=\omega_p/\sqrt{2}$, the slab is impedance matched with free space such that a decaying exponential becomes a growing exponential inside the BW slab and changes back into a decaying exponential on the other side of the slab as shown in Fig. 2. We will refer to such a wave form with vanishing reflected wave in the source region as a nonreflecting wave. The magnitude of the wave-vector components is spatially invariant because $\varepsilon\mu=1$ in all three regions. Consequently, the wave at $y=-a$, ($a<L$) in front of the slab is reproduced at $y=2L-a$ beyond the slab, independent of **k**; the BW slab compensates for the amplitude decay of the wave.[3] The slab also compensates for the phase propagation of a plane wave.[1] The combination of these two effects allows the perfect reconstruction of a point source as an image through a slab of BW material at frequency ω_0.[3]

As will be shown later, there are surface modes[7] whose frequencies are close to that of the nonreflecting wave [i.e., frequencies which cause the denominator of Eqs. (2) and (3) to be zero]. The change in permeability at the $y=0$ and $y=L$ interfaces allows them to support transverse-electric sur-

face waves. Surface waves in a single interface system decay exponentially away from the interface. The presence of other interfaces gives rise to coupling of the surface waves at each of the interfaces. This leads to the emergence of normal modes with slightly different frequencies. In the example system there are two such surfaces, and there exists a symmetric and an antisymmetric mode where the amplitude at one interface is equal to, or the negative of, the amplitude at the other interface, respectively. The modes do not couple to propagating waves but can be excited by evanescent waves. Due to their bound nature, they have a long decay time and can degrade the quality of the image of the source. Thus the structure is more suitable for steady-state rather than transient or time resolved operation.

It is more realistic to assume that the permittivity and the permeability change over a small transition layer from their free space values to the values in the BW material. When the thickness of this transition layer is finite the behavior of the fields becomes more complex. The finite transition layer shifts the frequency of the nonreflecting wave and of the surface modes. These shifts are dependent on the layer thickness and the normal component of the wave vector. The surface mode and nonreflecting wave frequencies are shown in Fig. 3 as a function of transition-layer thickness with transverse wavelengths $\lambda_t = 0.2\lambda_0$ and $\lambda_t = 0.8\lambda_0$. The nonreflecting wave frequency is bracketed by the two surface-mode frequencies. As the transition-layer thickness increases, all three frequencies shift upwards with the nonreflecting wave moving closer to the symmetric mode. The frequency shift is greater than the difference between them, even though the layer thickness is much less than the free space wavelength. Comparing the two cases depicted in Fig. 3, one finds that for the wave with the higher resolution ($\lambda_t = 0.2\lambda_0$) the frequencies of the surface modes and the nonreflecting wave are much closer to one another than in the case of the lesser resolution ($\lambda_t = 0.8\lambda_0$), so much so that the curves for $\lambda_t = 0.2\lambda_0$ are not distinguishable in the graph.

In Fig. 4 we show the frequencies of the two surface modes and the nonreflecting wave as a function of the transverse wavelength. In all cases, the symmetric surface mode has the highest frequency, while the antisymmetric one has the lowest frequency. The frequency of the nonreflecting wave lies between that of the two surface modes. At vanishing transition-layer thickness, the nonreflecting wave occurs at the design frequency ω_0, independent of the wave vector, while the surface mode frequencies change with the normal component of the wave vector. With a finite transition layer, the nonreflecting wave frequency also becomes dependent on the wave vector, as is shown in Fig. 4 with layer thickness $d = 0.005\lambda_0$. This wave vector dependence poses difficulties for the realization of a perfect lens.

The phase compensation of propagating waves inside the BW slab is independent of the wave vector only at the design frequency. In the transition layer, k_y is always imaginary for $\omega_s < \omega_p$, and phase does not propagate in these layers. Therefore the BW slab compensates for the change in phase due to propagation in free space from $y = -a$ $(a < L)$ at $y = 2L + 2d - a$. Thus for imaging application one has to look at the reconstruction of a source wave at the design frequency at this image location. The relative amplitude of the incident wave at the source location (E_{source}) and the transmitted amplitude at the image location (E_{image}) at the design frequency ω_0 is shown in Fig. 5 as a function of transverse wavelength. The expression for this relative amplitude is given by

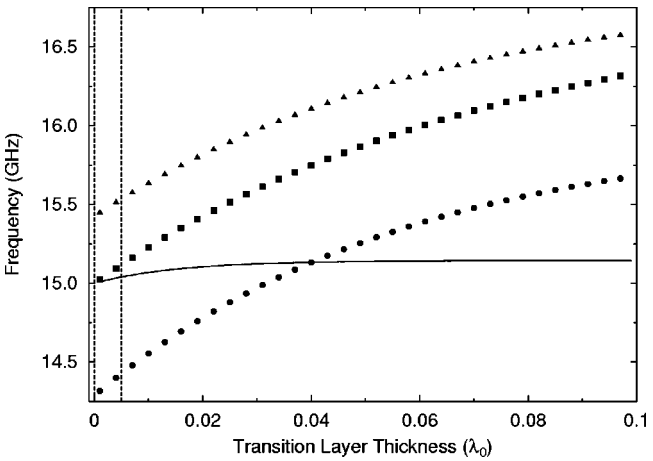

FIG. 3. Frequency of the nonreflecting wave (■), the antisymmetric (●), and the symmetric (▲) surface modes as a function of transition-layer thickness for transverse wavelength $\lambda_t = 0.8\lambda_0$. The frequencies for $\lambda_t = 0.2\lambda_0$ are shown by lines and have the same trends as the symbols but are not distinguishable on the scale of this plot. The dashed vertical lines indicate the transition layer thicknesses used in Fig. 4.

$$\frac{E_{\text{image}}}{E_{\text{source}}} = \frac{E_t}{E_i} e^{2ik_y^{11}(L+d)}, \tag{7}$$

which is the amplitude ratio of Eq. (3) adjusted for the locations according to Eq. (1). (Note that ik_y^{11} is real in this case.) The graph shows curves for several transition layer thicknesses. The relative amplitude exhibits singularities at the

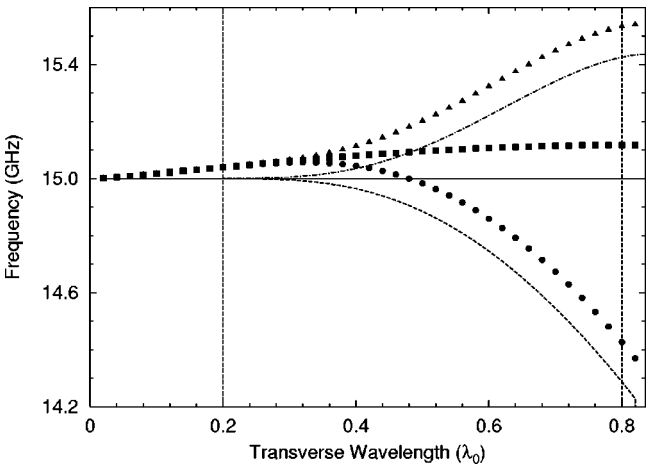

FIG. 4. Frequency of the nonreflecting wave (solid, ■), the antisymmetric (dashed, ●), and symmetric (dash-dot, ▲) surface modes as a function of transverse wavelength for transition-layer thickness $d = 0$ (lines) and $d = 0.005\lambda_0$ (symbols). The dashed vertical lines indicate the transverse wavelengths used in Fig. 3.

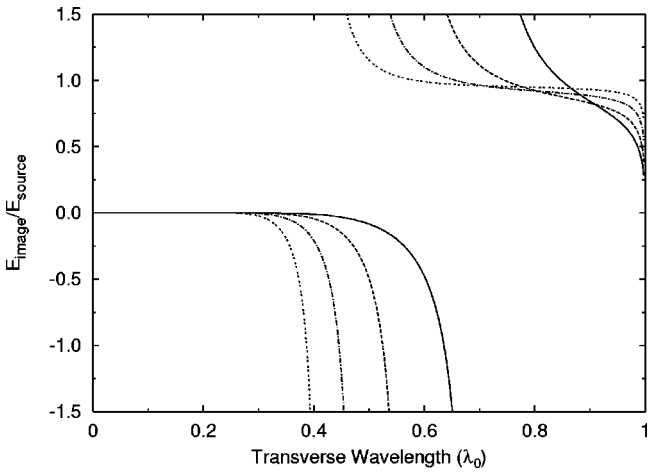

FIG. 5. Relative amplitude of the source electric field (E_{source}) amplitude at $y=-a=-3L/4$ and its image (E_{image}) at $y=2L-a+2d$ with a transition layer of $d=0.02\lambda_0$ (solid), $0.01\lambda_0$ (dashed), $0.005\lambda_0$ (dash-dot), and $0.0025\lambda_0$ (dash-dashed) at the design frequency ω_0 as a function of transverse wavelength λ_t. The singularities are caused by the antisymmetric surface mode, i.e., $E_{\text{source}}=0$.

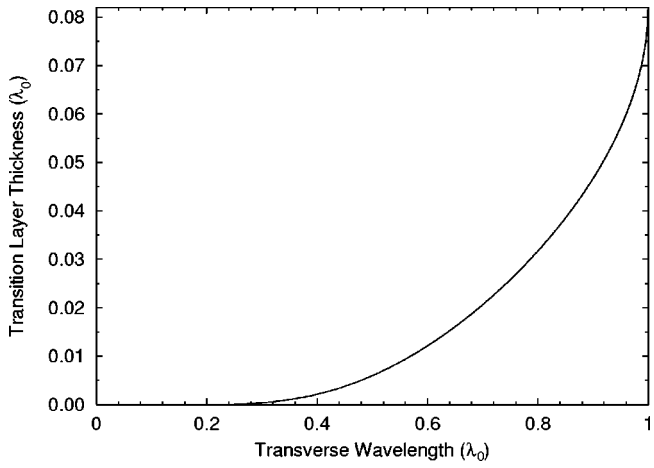

FIG. 6. Layer thickness where the antisymmetric surface mode occurs as a function of transverse wavelength. (The curve on this graph begins at $\lambda_t=0.251\lambda_0$ with $d=0.0001\lambda_0$. Smaller values of λ_t were not accessible due to the finite numerical precision when evaluating the expression for the surface mode.)

occurrence of the antisymmetric surface mode, because the incident wave, which is proportional to the denominator in this ratio, vanishes. With larger values of L the surface mode shifts to greater λ_t. For λ_t greater than that of the antisymmetric surface mode, one finds a region in λ_t where the ratio of image amplitude and source amplitude is close to unity. The extent of this region increases with decreasing transition-layer thickness. For smaller transverse wavelength the relative amplitude vanishes rapidly with decreasing λ_t. (In steady state the surface mode has no associated incident wave. An incident wave whose frequency and wave vector correspond to that of the surface mode would continuously pump the mode. This would lead to the surface mode drowning out the image of the source.) The surface mode clearly acts as a lower bound on the feature size of the source that can be resolved with a given system. To illustrate this, Fig. 6 shows the relationship between the transition-layer thickness and the transverse wavelength at which the antisymmetric surface mode occurs. The graph shows that as one reduces the transition-layer thickness, the limiting transverse wavelength decreases as well, thus increasing resolution. The relationship between d and λ_t is approximately cubic in the region of the graph. Thus, a reduction of d accomplishes a much smaller reduction of λ_t and makes the quest for higher resolution with this system expensive.

V. CONCLUSION

We have presented a study of evanescent wave behavior in a BW material and specifically considered the influence of a dielectric transition layer between a BW slab and free space. A vanishing transition layer can give the ideal case with perfect reconstruction of a point source, while transition layers much thinner than the free-space wavelength of the radiation give rise to a surface mode at the design frequency. This surface mode acts as a lower bound on the correctly imaged transverse wavelength. The influence of the transition layers on propagating waves is less pronounced than on evanescent waves. The significance of transition layers much smaller than the free space wavelength for evanescent waves, as shown in this study, suggests that the use of a macroscopic ε and μ may not be appropriate at an interface of forward-wave and backward-wave materials.[8] Nevertheless, this study gives important insight into the behavior of BW materials and shows promise for imaging beyond the diffraction limit but also points out difficulties in the structure and the modeling of these materials.

ACKNOWLEDGMENTS

We would like to thank Richard Ziolkowski for useful discussion. This work was supported by the Office of Naval Research code 321OA.

[1] V.G. Veselago, Usp. Fiz. Nauk **92**, 517 (1967) [Sov. Phys. Usp. **10**, 509 (1968)].
[2] D.R. Smith, W.J. Padilla, D.C. Vier, S.C. Nemat-Nasser, and S. Schultz, Phys. Rev. Lett. **84**, 4184 (2000).
[3] J.B. Pendry, Phys. Rev. Lett. **85**, 3966 (2000).
[4] R.W. Ziolkowski and E. Heyman, Phys. Rev. E **64**, 056625 (2001).
[5] R.A. Shelby, D.R. Smith, and S. Schultz, Science **292**, 77 (2001).
[6] R.A. Shelby, D.R. Smith, S.C. Nemat-Nasser, and S. Schultz, Appl. Phys. Lett. **78**, 489 (2001).
[7] R. Ruppin, J. Phys.: Condens. Matter **13**, 1811 (2001).
[8] T. Weiland, R. Schuhmann, R.B. Greegor, C.G. Parazzoli, A.M. Vetter, D.R. Smith, D.C. Vier, and S. Schultz, J. Appl. Phys. **90**, 5419 (2001).